Piezoelectricity in $K_{1-x}Na_xNbO_3$: First-principles calculation*

Li Qiang(李 强), Zhang Rui(张 锐)†, Lv Tian-Quan(吕天全)‡, and Zheng Li-Mei(郑立梅)

Condensed Matter Science and Technology Institute, Harbin Institute of Technology, Harbin 150080, *China*

(Received 15 September 2014; revised manuscript received 8 December 2014; published online 27 March 2015)

The piezoelectric properties of $K_{1-x}Na_xNbO_3$ are studied by using first-principles calculations within virtual crystal approximation. To understand the critical factors for the high piezoelectric response in $K_{1-x}Na_xNbO_3$, the total energy, piezoelectric coefficient, elastic property, density of state, Born effective charge, and energy barrier on polarization rotation paths are systematically investigated. The morphotropic phase boundary in $K_{1-x}Na_xNbO_3$ is predicted to occur at $x = 0.521$, which is in good agreement with the available experimental data. At the morphotropic phase boundary, the longitudinal piezoelectric coefficient d_{33} of orthorhombic $K_{0.5}Na_{0.5}NbO_3$ reaches a maximum value. The rotated maximum of d^*_{33} is found to be along the 50° direction away from the spontaneous polarization (close to the [001] direction). The moderate bulk and shear modulus are conducive to improving the piezoelectric response. By analyzing the energy barrier on polarization rotation paths, it is found that the polarization rotation of orthorhombic $K_{0.5}Na_{0.5}NbO_3$ becomes easier compared with orthorhombic $KNbO_3$, which proves that the high piezoelectric response is attributed to the flattening of the free energy at compositions close to the morphotropic phase boundary.

Keywords: first principles, morphotropic phase boundary, piezoelectricity, virtual crystal approximation

PACS: 31.15.A–, 77.65.–j, 77.84.Cg **DOI:** 10.1088/1674-1056/24/5/053101

1. Introduction

Lead-based piezoelectric materials have been widely used in sensors, actuators, and accelerometers.[1] However, due to Pb's toxicity, there is an increasing attention in the development of high-performance lead-free piezoelectric materials. Environmentally friendly (K, Na)NbO_3 (KNN) and its solid solutions show the superior piezoelectric properties at a K/Na ratio of around 50/50, and are the potential substitutes for lead-based piezoelectrics.[2–7] It is well known that the piezoelectric response is enhanced for piezoelectrics at the morphotropic phase boundary (MPB).[1,8] Therefore, a great deal of experimental effort has been devoted to search the MPB composition in the $K_{1-x}Na_xNbO_3$ system. Studies[9–12] on the phase transition process in the KNN system suggested that an MPB lies near the composition with 50 mol.% $NaNbO_3$. In those studies, the Na content intervals are too large to verify the accurate K/Na ratio at the MPB. The small intervals in $K_{1-x}Na_xNbO_3$ ceramics have been derived by Dai *et al.*[13] Their results suggested that a typical morphotropic phase boundary exists at $x = 0.52$–0.525. Although the accurate MPB in $K_{1-x}Na_xNbO_3$ has been confirmed experimentally, some fundamental problems still need to be solved, such as the dominant factor for the high piezoelectric response in $K_{1-x}Na_xNbO_3$, the effect of K–O (or Na–O) and Nb–O bonding on the piezoelectric performance, and the effect of Na substitution on the polarization rotation. First-principles calculations can predict various properties well,[14–18] such as the phase transition and thermodynamic properties, which have been adopted for the purpose of this report.

In this paper, we use first-principles density functional theory within the virtual crystal approximation to predict the MPB in $K_{1-x}Na_xNbO_3$ and evaluate its piezoelectric response behaviors. Moreover, the mechanism of a high piezoelectric response and the effect of the domain-engineering method on polarization rotation in $K_{1-x}Na_xNbO_3$ near the MPB are also investigated. To the best of our best knowledge, it is the first time that the MPB of KNN has been obtained theoretically. This paper is organized as follows. Theoretical methods are described in Section 2. The results for the structural parameter, bulk modulus, band gap, Born dynamical charge, and piezoelectric property are discussed in Section 3. Finally, the conclusions are given in Section 4.

2. Computational methods

The first-principles calculations are conducted using the density functional theory (DFT) and plane wave pseudopotential method implemented in the ABINIT software package.[19–22] In order to quantitatively investigate the MPB and related phenomena, the virtual crystal approximation (VCA)[23] is adopted because it has been successfully applied to some perovskite solutions (e.g., PZT,[24,25] NBT-BT,[26] PSN,[27] and LNTO[28]). The exchange correlation potential is described by the local-density approximation within the Hartwigsen–Goedecker–Hutter (HGH) pseudopotentials.[29] We treat 9 valence electrons for K ($3s^23p^64s^1$) and Na ($2s^22p^63s^1$), 6 for O ($2s^22p^4$), and 13 for Nb ($4s^24p^64d^45s^1$).

*Project supported by the National Basic Research Program of China (Grant No. 2013CB632900).

†Corresponding author. E-mail: ruizhang_ccmst@hit.edu.cn

‡Corresponding author. E-mail: ltq@hit.edu.cn

© 2015 Chinese Physical Society and IOP Publishing Ltd

The Brillouin zone (BZ) is sampled by a 5×5×5 Monkhorst–Pack mesh of k points for cubic, rhombohedra, orthorhombic, and tetragonal $K_{1-x}Na_xNbO_3$. To achieve high accuracy in the total energy calculation and ionic relaxation, we use a very high plane-wave energy cutoff of 3591 eV, and the convergence for the maximum tolerance on the wave function squared residual is set to 10^{-18}. Firstly, the appropriate cell parameters of $K_{1-x}Na_xNbO_3$ are obtained after optimizing the lattice constants and internal atom coordinates based on the maximal force tolerance (0.0257 eV/Å). Secondly, the total energy, piezoelectric constant, Born effective charge, and elastic property calculations for $K_{1-x}Na_xNbO_3$ are performed by the density functional perturbation theory (DFPT).[30]

3. Results and discussion

3.1. Structure properties

Above the Curie temperature (around 624 K), $KNbO_3$ (KNO) is a typical perovskite structure with the cubic symmetry. Cooling KNO from the Curie temperature leads to a continuous phase transition in a cubic-tetragonal-orthorhombic-rhombohedral sequence. The calculated lattice parameter, bulk modulus, and band gap for these phases are presented in Table 1. The lattice constant a and the cell volume V of the cubic phase are calculated to be 3.968 Å and 62.46 Å^3, respectively, which are in good agreement with the experimental values (4.021 Å and 65.01 Å^3).[32] The calculated c/a ratio for the tetragonal KNO is 1.034, which agrees with the available experimental result (1.017).[36] According to the present DFT calculations, the unit-cell parameters of $a = 5.629$ Å, $b = 3.959$ Å, and $c = 5.633$ Å are predicted for the orthorhombic KNO. The rhombohedral KNO with the space group $R3m$ only exists below room temperature.

Table 1. Lattice parameter, volume, bulk modulus, band gap, and piezoelectric constant of the cubic, tetragonal, orthorhombic, and rhombohedral $KNbO_3$, compared with experimental and theoretical data. For each phase, the error of lattice parameter with respect to the experimental data is given.

	Calc.	Other	Exp.	Error	
Cubic	a/Å	3.968	3.960[a]	4.021[b]	1.3%
	V/Å^3	62.46	62.10[a]	65.01[b]	
	B/GPa	132	182[c]	138[d]	
	E_g/eV	2.160			
Tetragonal	a/Å	3.963	3.939[e]	3.996[f]	0.8%
	c/Å	3.997	3.983[e]	4.063[f]	1.6%
	V/Å^3	62.76	61.80[e]	64.88[f]	
	B/GPa	194	143[c]		
	E_g/eV	2.127			
	d_{33}/pC·N^{-1}	40.0	38.9[c]		
Orthorhombic	a/Å	5.629	5.744[c]	5.697[g]	1.2%
	b/Å	3.959	3.980[c]	3.971[g]	0.3%
	c/Å	5.633	5.771[c]	5.721[g]	1.5%
	V/Å^3	125.54	65.97[c]	129.42[g]	
	B/GPa	185	127[c]	172[h]	
	E_g/eV	2.210			
	d_{33}/pC·N^{-1}	24.3	20.07[c]	24.5[i]	
Rhombohedral	a/Å	3.975	4.041[c]	4.016[f]	1.00%
	α/(°)	89.96	89.85[c]	89.82[f]	0.16%
	V/Å^3	62.80	65.96[c]	64.77[f]	
	B/GPa	197	118[c]		
	E_g/eV	2.272			
	d_{33}/pC·N^{-1}	14.7	10.8[c]		

[a]Ref. [31], [b]Ref. [32], [c]Ref. [33], [d]Ref. [34], [e]Ref. [35], [f]Ref. [36], [g]Ref. [37], [h]Ref. [38], [i]Ref. [39].

Compared with the reported experimental data,[32,36,37] our calculated cell parameters listed in Table 1 have an accuracy with a relative error of ±1.6%. The predicted bulk modulus for the cubic and orthorhombic KNO are 132 GPa and 185 GPa, respectively, which are consistent with the experimental data (138 GPa and 172 GPa).[34,38] The calculated piezoelectric coefficients d_{33} are also in reasonable agreement with the experimental and theoretical data.[33,39]

3.2. Morphotropic phase boundary

The aim of our study is to predict the MPB in $K_{1-x}Na_xNbO_3$. Thus, the total energy differences of the rhombohedral, orthorhombic, and tetragonal $K_{1-x}Na_xNbO_3$ as a function of Na content are calculated and shown in Fig. 1. As seen in Fig. 1, the energy of the rhombohedral $K_{1-x}Na_xNbO_3$ with a low content of Na ($x < 0.521$) is found to be lower than that of the orthorhombic and tetragonal structures, which indicates that the rhombohedral $K_{1-x}Na_xNbO_3$ is more stable under the Na-poor (K-rich) condition. With the increase of Na content ($0.8 > x > 0.521$), the energy of the orthorhombic phase becomes lower than that of the rhombohedral one. Thus, in this content range, the orthorhombic $K_{1-x}Na_xNbO_3$ is more stable than both the rhombohedral and tetragonal structures. If the two phases have the same energy, these two phases may coexist in this region. From Fig. 1, the energies of the rhombohedral and orthorhombic $K_{1-x}Na_xNbO_3$ are equal at $x = 0.521$, which confirms an MPB in $K_{1-x}Na_xNbO_3$. This prediction is in good agreement with the experimental data ($x = 0.52$–0.525).[13] At $x = 0.9$, a big leap in the total energy of the orthorhombic phase can be observed. According to the $K_{1-x}Na_xNbO_3$ phase diagram,[40] we can understand that the $K_{1-x}Na_xNbO_3$ shows different structures in this region ($x = 0.9$), e.g., monoclinic and orthorhombic phases, leading to significant changes in the energy of the orthorhombic phase. Thus, the first-principles calculation within the VCA, which only requires the knowledge of the atom number and crystal structure, is a very effective tool in theoretical prediction of MPB.

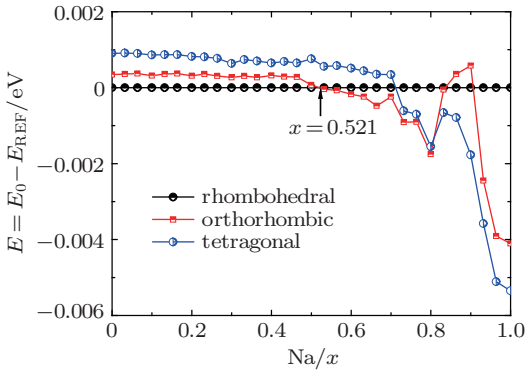


Fig. 1. (color online) Calculated energy as a function of Na content (x) for the rhombohedral, orthorhombic, and tetragonal $K_{1-x}Na_xNbO_3$. Here we subtract the energy $E_{\rm REF}$ of the rhombohedral $K_{1-x}Na_xNbO_3$ from the energy E_0 of each phase.

3.3. Piezoelectric properties

At the MPB, the piezoelectric materials would show the high piezoelectric properties. In order to further verify our prediction, we calculate the piezoelectric coefficients (d_{33} and d_{15}). Figure 2 only shows d_{33} of the orthorhombic $K_{1-x}Na_xNbO_3$ in the range of $x = 0.0$–0.7, because the elastic constant calculations suggest that the orthorhombic $K_{1-x}Na_xNbO_3$ becomes mechanically instable in the range of $x > 0.7$. The d_{33} of the orthorhombic structure shows a maximum value at $x = 0.5$. This result is in agreement with the experimental measurements.[9–12] The reason for the peak value at $x = 0.2$ is unclear yet. There may be another MPB or phase boundary. Similarly, the d_{33} also shows a maximum at $x = 0.2$ in both $BiFe_{1-x}Co_xO$ and $(NBT)_{1-x}$-$(K_{1/2}BiTiO_3)_x$, which has been thoroughly verified by the experimental[41–43] and theoretical[44] studies.

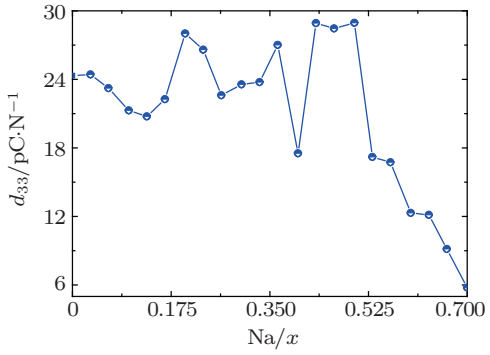


Fig. 2. (color online) d_{33} of the orthorhombic $K_{1-x}Na_xNbO_3$ as a function of x.

The shear piezoelectric coefficient d_{15} is also very important for piezoelectrics. Therefore, we calculate d_{15} as a function of x for the orthorhombic $K_{1-x}Na_xNbO_3$. As shown in Fig. 3, there are three peaks located at $x = 0.2$, 0.464, and 0.7. Although d_{15} at $x = 0.7$ is the highest among the three peaks, the corresponding d_{33} is the lowest. At x= 0.464, d_{15} is calculated to be 153.52 pC/N, which further identifies the MPB in $K_{1-x}Na_xNbO_3$.

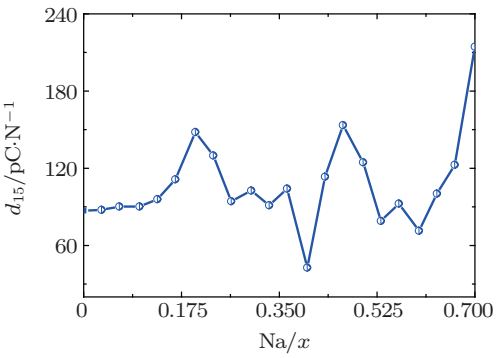


Fig. 3. (color online) d_{15} of the orthorhombic $K_{1-x}Na_xNbO_3$ as a function of x.

3.4. Orientation dependence of piezoelectric coefficient

According to the suggestion of Davis *et al.*,[45] the largest longitudinal piezoelectric response would be found away from the polar direction when the ratio d_{15}/d_{33} is larger than 1.5, and the crystals can be categorized into "rotator" ferroelectrics with $d_{15}/d_{33} > 1.5$ and "extender" with $d_{15}/d_{33} < 1.5$. According to the predicted piezoelectric coefficients d_{33} and d_{15}, the d_{15}/d_{33} value is 7.29 for the orthorhombic $K_{0.5}Na_{0.5}NbO_3$. Thus, the orthorhombic $K_{0.5}Na_{0.5}NbO_3$ belongs to "rotator" ferroelectrics and is highly anisotropic. The large anisotropy is also observed in other single-domain relaxor-PT-based crystals near their MPBs.[8] It is necessary for investigating the crystal orientation dependence of the piezoelectric properties. From the calculated single-domain data of the orthorhombic $K_{1-x}Na_xNbO_3$ with $x = 0.5$ and 0.0, the orientation dependence of the intrinsic piezoelectric coefficient d_{33}^* is calculated through the transformation of the single domain piezoelectric matrix,[8,46,47] and the results are presented in Fig. 4. One can see that the highest value of the piezoelectric coefficient d_{33}^* of the orthorhombic $K_{1-x}Na_xNbO_3$ with $x = 0.5$ is on the order of 58.4 pC/N, being along the $\theta_{\rm max} = 50°$ away from the spontaneous polarization [011] direction (close to the [001] direction), larger than that with $x = 0.0$. Thus, the piezoelectric coefficients d_{33}^* exhibit strong orientation dependence.

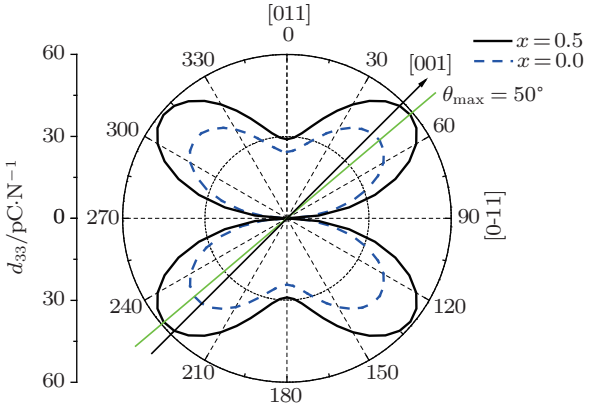


Fig. 4. (color online) Orientation dependence of piezoelectric coefficient d_{33}^* of the orthorhombic $K_{1-x}Na_xNbO_3$ with $x = 0.5$ and $x = 0.0$.

3.5. Bulk modulus and shear modulus

For the orthorhombic $K_{1-x}Na_xNbO_3$ with $x = 0.5$, there are nine independent elastic constants (c_{11}, c_{22}, c_{33}, c_{44}, c_{55}, c_{66}, c_{12}, c_{13}, and c_{23}), which are obtained using DFPT. From the calculated elastic constants, both the bulk modulus (B) and shear modulus (G) can be derived using Voigt–Reuss–Hill (VRH) approximation,[48] and the results are presented in Fig. 5. The VRH bulk modulus is defined as the average $B = (B_V + B_R)/2$ between the Voigt upper and Reuss lower bounds

$$B_V = \frac{1}{9}(c_{11}+c_{22}+c_{33}) + \frac{2}{9}(c_{12}+c_{13}+c_{23}), \quad (1)$$

$$B_R = \frac{1}{(s_{11}+s_{22}+s_{33}) + 2(s_{12}+s_{13}+s_{23})}. \quad (2)$$

The VRH shear modulus $G = (G_V + G_R)/2$ is taken from the average between the Voigt upper G_V and Reuss lower G_R bounds

$$G_V = \frac{1}{15}(c_{11}+c_{22}+c_{33}-c_{12}-c_{13}-c_{23}) + \frac{1}{5}(c_{44}+c_{55}+c_{66}), \quad (3)$$

$$G_R = 15/[4(s_{11}+s_{22}+s_{33}) - 4(s_{12}+s_{13}+s_{23}) + 3(s_{44}+s_{55}+s_{66})]. \quad (4)$$

From Fig. 5, three minimum value of the bulk B and shear G modulus are located at $x = 0.2$, 0.464, and 0.7. The bulk B and shear G modulus at $x = 0.7$ are the smallest among the three minimum values. The corresponding d_{33} is also the smallest, as shown in Fig. 2. This implies that the small bulk and shear modulus would not necessarily give rise to a high piezoelectric response. Otherwise, the exceptionally high bulk and shear modulus are also not conducive to a high piezoelectric response. Therefore, the moderate bulk and shear modulus are better for the piezoelectric response.

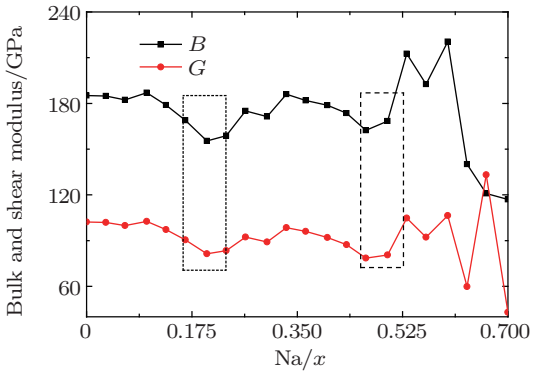


Fig. 5. (color online) Bulk and shear modulus of the orthorhombic $K_{1-x}Na_xNbO_3$ as a function of x.

3.6. Partial density of state

The first-principles studies have suggested that the orbital hybridization between the Pb 6s state and O 2p states plays a crucial role for large ferroelectricity in tetragonal $PbTiO_3$.[49] The prediction is later verified experimentally,[50] i.e., the Pb–O bonds in tetragonal $PbTiO_3$ show rather strong covalency. In order to investigate the interaction between Nb–O and K–O bonds, we plot the partial density of state (PDOS) of the Nb, K, and O orbitals for the orthorhombic $K_{1-x}Na_xNbO_3$ with $x = 0.5$. As shown in Fig. 6, the K 2s and 2p, O 2p orbits are mainly located in the range from −5.6 to 0 eV, indicating that the K–O bonds are mainly ionic. The calculated Born effective charge of K is 1.13, which is close to its oxidation state, further confirming the characteristic of ionic interaction between K and O ions. The Nb 4d orbits mixed with O 2p orbits are located in the valence band and conduction band, suggesting that the Nb–O bonds are both ionic and covalent. The calculated average Born effective charge of Nb is 8.79, larger than its oxidation state (+5), indicating that the Nb–O bonds are not purely ionic. Thus, the high piezoelectric for orthorhombic $K_{1-x}Na_xNbO_3$ with $x = 0.5$ is related to the Nb–O covalency. This agrees with the recent theoretical study.[51]

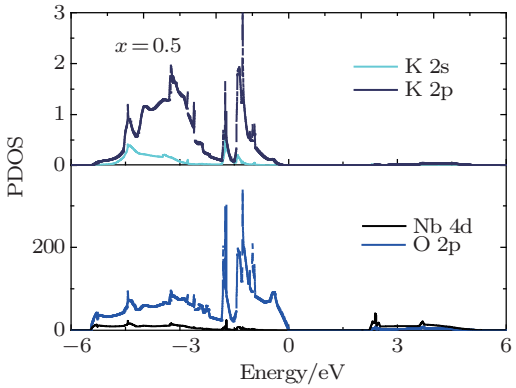


Fig. 6. (color online) Partial density of state of the orthorhombic $K_{1-x}Na_xNbO_3$.

3.7. Energy barrier on polarization rotation paths

To understand the physical mechanism of the high piezoelectric response for the orthorhombic $K_{1-x}Na_xNbO_3$, we calculate the energy barrier on polarization rotation paths along the [001] direction through a simple approach: $E(\theta) = E_0(\theta) - E_0(0)$, where $E(\theta)$ is the energy barrier with θ being the angle of polarization rotation, $E_0(\theta)$ is the total energy of the orthorhombic $K_{1-x}Na_xNbO_3$, and $E_0(0)$ denotes the total energy with $\theta = 0°$. The adopted model for the energy barrier calculations is illustrated in Fig. 7, and the results are depicted in Fig. 8. As shown in Fig. 8, the energy barrier of the orthorhombic $K_{1-x}Na_xNbO_3$ with x = 0.0 and $x = 0.5$ increases with the increase of the angle θ. However, the energy barrier of the orthorhombic $K_{1-x}Na_xNbO_3$ with x = 0.5 increases more slowly than the one with $x = 0.0$, indicating that at MPB, the phase instability of the orthorhombic $K_{1-x}Na_xNbO_3$ with $x = 0.5$ is enhanced and the polarization rotation becomes easier than the pure KNO, i.e., the flat free

energy profile is the most important factor for inducing a high piezoelectric response.

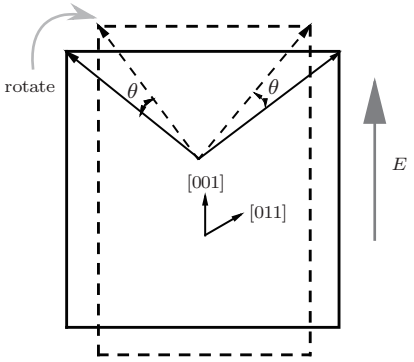


Fig. 7. Schematic of polarization rotation of the orthorhombic $K_{1-x}Na_xNbO_3$ resulting from [001] electric field.

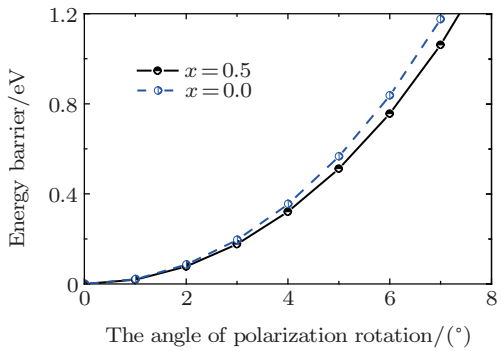


Fig. 8. (color online) Energy barrier of the orthorhombic $K_{1-x}Na_xNbO_3$ with $x = 0.5$ and 0.0 on polarization rotation paths along the [001] direction.

4. Conclusions

First-principles density functional theory within the virtual crystal approximation is applied to investigate the morphotropic phase boundary and piezoelectric properties of $K_{1-x}Na_xNbO_3$. The structure parameter, bulk modulus, band gap, and piezoelectric coefficients have been calculated. The MPB in $K_{1-x}Na_xNbO_3$ is predicted to be located at $x = 0.521$, which is in good agreement with the experimental data. The dependence of the longitudinal piezoelectric coefficient on the polarization orientation proves that the highest value of the piezoelectric coefficient d^*_{33} of the orthorhombic $K_{1-x}Na_xNbO_3$ with $x = 0.5$ is close to the [001] direction. According to the comparison of the energy barrier of polarization rotation from [011] to [001] direction, we prove that the polarization rotation for $K_{0.5}Na_{0.5}NbO_3$ becomes easier at MPB, and a flat free-energy is the most important factor for high piezoelectricity. The present calculation also provides a way to predict the MPB in lead-free piezoelectric materials.

References

[1] Sun E and Cao W 2014 *Prog. Mater. Sci.* **65** 124
[2] Gao Y, Zhang J, Zong X, Wang C and Li J 2010 *J. Appl. Phys.* **107** 074101
[3] Guo Y, Kakimoto K I and Ohsato H 2004 *Solid State Commun.* **129** 279
[4] Hollenstein E, Davis M, Damjanovic D and Setter N 2005 *Appl. Phys. Lett.* **87** 182905
[5] Shrout T R and Zhang S J 2007 *J. Electroceram.* **19** 113
[6] Zhang J, Zong X, Wu L, Gao Y, Zheng P and Shao S 2009 *Appl. Phys. Lett.* **95** 022909
[7] Saito Y, Takao H, Tani T, Nonoyama T, Takatori K, Homma T, Nagaya T and Nakamura M 2004 *Nature* **432** 84
[8] Zhang S and Li F 2012 *J. Appl. Phys.* **111** 031301
[9] Wang R, Xie R-J, Hanada K, Matsusaki K, Bando H, Sekiya T and Itoh M 2006 *Ferroelectrics* **336** 39
[10] Tennery V J and Hang K W 1968 *J. Appl. Phys.* **39** 4749
[11] Zhang B P, Li J F, Wang K and Zhang H 2006 *J. Am. Ceram. Soc.* **89** 1605
[12] Jaeger R E and Egerton L 1962 *J. Am. Ceram. Soc.* **45** 209
[13] Dai Y J, Zhang X W and Chen K P 2009 *Appl. Phys. Lett.* **94** 042905
[14] Li Q, Huang D H, Cao Q L and Wang F H 2013 *Chin. Phys. B* **22** 037101
[15] Luo F, Cheng Y, Cai L C and Chen X R 2013 *J. Appl. Phys.* **113** 033517
[16] Ao B-Y, Shi P, Guo Y and Gao T 2013 *Chin. Phys. B* **22** 037103
[17] Guo Y, Ai J J, Gao T and Ao B Y 2013 *Chin. Phys. B* **22** 057103
[18] Hu C, Wang F, Xia C, Zheng Z and Ren W 2011 *Mod. Phys. Lett. B* **25** 333
[19] Gonze X, Rignanese G M, Verstraete M, Beuken J M, Pouillon Y, Caracas R, Jollet F, Torrent M, Zerah G, Mikami M, Ghosez P, Veithen M, Raty J Y, Olevano V, Bruneval F, Reining L, Godby R, Onida G, Hamann D R and Allan D C Z 2005 *Kristallogr.* **220** 558
[20] Gonze X, Amadon B, Anglade P M, Beuken J M, Bottin F, Boulanger P, Bruneval F, Caliste D, Caracas R and Cote M 2009 *Comput. Phys. Commun.* **180** 2582
[21] Gonze X and Lee C 1997 *Phys. Rev. B* **55** 10355
[22] Hamann D, Wu X, Rabe K M and Vanderbilt D 2005 *Phys. Rev. B* **71** 035117
[23] Bellaiche L and Vanderbilt D 2000 *Phys. Rev. B* **61** 7877
[24] Ramer N J and Rappe A M 2000 *Phys. Rev. B* **62** R743
[25] Liu S Y, Shao Q S, Yu D S, Lv Y K, Li D J, Li Y and Cao M S 2013 *Chin. Phys. B* **22** 17702
[26] Deng Y, Wang R Z, Xu L C, Fang H, Yang X, Yan H and Chu P K 2011 *Appl. Phys. A* **104** 1085
[27] Haumont R, Dkhil B, Kiat J, Al-Barakaty A, Dammak H and Bellaiche L 2003 *Phys. Rev. B* **68** 014114
[28] Geneste G, Kiat J M and Malibert C 2008 *Phys. Rev. B* **77** 052106
[29] Hartwigsen C, Goedecker S and Hutter J 1998 *Phys. Rev. B* **58** 3641
[30] Wu X, Vanderbilt D and Hamann D 2005 *Phys. Rev. B* **72** 035105
[31] Wu Z, Cohen R and Singh D 2004 *Phys. Rev. B* **70** 104112
[32] Shirane G, Newnham R and Pepinsky R 1954 *Phys. Rev.* **96** 581
[33] Wan L, Nishimatsu T and Beckman S 2012 *J. Appl. Phys.* **111** 104107
[34] Wiesendanger E 1973 *Ferroelectrics* **6** 263
[35] Shigemi A and Wada T 2005 *Jpn. J. Appl. Phys.* **44** 8048
[36] Hewat A 1973 *J. Phys. C: Solid State Phys.* **6** 2559
[37] Katz L and Megaw H 1967 *Acta Cryst.* **22** 639
[38] Kalinichev A G, Bass J D, Zha C S, Han P D and Payne D A 1993 *J. Appl. Phys.* **74** 6603
[39] Günter P 1977 *Jpn. J. Appl. Phys.* **16** 1727
[40] Jaffe B 2012 *Piezoelectric Ceramics*, Vol. 3 (Elsevier)
[41] Nakamura Y, Kawai M, Azuma M and Shimakawa Y 2010 *Jpn. J. Appl. Phys.* **49** 051501
[42] Hiruma Y, Nagata H and Takenaka T 2008 *J. Appl. Phys.* **104** 124106
[43] Royles A, Bell A, Jephcoat A, Kleppe A, Milne S and Comyn T 2010 *Appl. Phys. Lett.* **97** 132909
[44] Kaoru M, Makoto K, Masaki A and Hiroshi F 2010 *Jpn. J. Appl. Phys.* **49** 09ME07
[45] Davis M, Budimir M, Damjanovic D and Setter N 2007 *J. Appl. Phys.* **101** 054112
[46] Li F, Zhang S, Xu Z, Wei X, Luo J and Shrout T R 2010 *J. Am. Ceram. Soc.* **93** 2731
[47] Liu X, Zhang S, Luo J, Shrout T R and Cao W 2010 *Appl. Phys. Lett.* **96** 012907
[48] Hill R 1963 *J. Mech. Phys. Solid.* **11** 357
[49] Cohen R E 1992 *Nature* **358** 136
[50] Kuroiwa Y, Aoyagi S, Sawada A, Harada J, Nishibori E, Takata M and Sakata M 2001 *Phys. Rev. Lett.* **87** 217601
[51] Shi J, Grinberg I, Wang X and Rappe A M 2014 *Phys. Rev. B* **89** 094105